Understanding core-level decay processes in the high-temperature superconductors

D. E. Ramaker and N. H. Turner
Chemistry Division, Naval Research Laboratory, Washington, D.C. 20375

F. L. Hutson
Department of Chemistry, George Washington University, Washington, D.C. 20052
(Received 9 August 1988)

A highly correlated CuO_n cluster model is utilized to interpret the core-level Auger and x-ray emission decay spectra for $YBa_2Cu_3O_{7-x}$ and CuO. The evidence indicates that the initial core-level shakeup states relax to states of the same symmetry before the core-level decay, provided they have a shakeup excitation energy much greater than the core-level width.

Previously reported[1,2] core-level Auger-electron spectroscopy (AES) and x-ray-emission spectroscopy (XES) data are interpreted within a highly correlated CuO_n cluster model for the high-temperature superconductors (HTSC's), $YBa_2Cu_3O_{7-x}$ and $La_{2-x}Ba_xCuO_4$ (herein referred to as 1:2:3 and La). The $L_{23}M_{23}V$ Auger line shape is reported here for the first time and is interpreted consistently with the $L_{23}VV$ line shape and XES data. This work clearly indicates, contrary to previous reports,[1,3] that the initial-core shakeup (ICSU) states do not directly decay, but rather relax to the primary core state before decay. The XES data dramatically reveal the change of character of the valence-band (VB) states between CuO and the1:2:3 material.

The basic electronic structure of the HTSC's can be described within the Anderson Hamiltonian utilized by Sawatzky and co-workers.[3,4] It includes the transfer or hopping integral t, the Cu and O orbital energies ε_d and ε_p, the core polarization energy Q_d, and the intrasite Coulomb repulsion energies U_d and U_p (the latter sometimes assumed to be zero). This model is most useful when the U's are large relative to the bandwidths,[3] i.e., when correlation effects dominate hybridization effects. A $CuO_n^{(2n-2)-}$ cluster model, which is also reasonably valid when $U \gg t$, simplifies the model further.[3] We utilize an extended Hubbard model by adding the intersite repulsion energies U_{dp} and U_{pp^o} (i.e., between neighboring Cu-O and O-O atoms). The addition of these interactions is important for understanding many of the features in the AES and XES data. The optimal U and ε parameters previously reported for the HTSC's (Refs. 4–6) were obtained empirically from the Cu $2p$ x-ray photoemission spectroscopy (XPS) and the VB ultraviolet photoemission spectroscopy (UPS) data utilizing the Anderson model. Our optimal extended Hubbard parameters in Table I were obtained by considering this same data plus x-ray-absorption spectroscopy (XAS) data,[7] and the Auger and XES data discussed in this work. Although we are in general agreement with the reported magnitudes for most of the parameters, our U_d value is larger by about 2–3 eV to be consistent with the AES data.

The $CuO_n^{(2n-2)-}$ cluster has one hole shared between the Cu $3d$ and O $2p$ shells in the ground state, which we term the v (valence) states. The spectroscopic final states reflect multihole states, e.g., v^2, cv (c=core), etc. We indicate the location of the v holes by d (Cu $3d$) or p (O $2p$). In the case of two holes on the oxygens, we distinguish two holes on the same O (p^2), on ortho neighboring O atoms (pp^o), or on para O atoms (pp^p) of the cluster. Furthermore, neighboring pp^o holes can dimerize,[8] so we distinguish between two holes in bonded (pp^{o_b}) and antibonded (pp^{o_a}) O pairs.[7]

The v states, as reflected by the theoretical density of states (DOS),[9] have the Cu–O bonding (Ψ_b) and antibonding (Ψ_a) orbitals centered at 4 and 0 eV, respectively, and the nonbonding Cu and O orbitals at 2 eV. The O features each have a width $2\Gamma = 4$ eV due to the O–O bonding and antibonding character and the Cu-O dispersion. The Ψ_b and Ψ_a wave functions can be expressed as[3]

$$\Psi_a = d\cos\theta_1 - p\sin\theta_1 , \tag{1a}$$

$$\Psi_b = d\sin\theta_1 + p\cos\theta_1 , \tag{1b}$$

where $\theta_1 = 0.5\tan^{-1}(2t/\Delta)$. We also define the Cu-O hybridization shift $\delta_1 = [(\Delta^2+4t^2)^{1/2}-\Delta]/2$, which is utilized in Table I to give the energies. Thus, the ground state of an average CuO_n cluster is located at 1 eV having the energy $\varepsilon_d - \delta_1 + \Gamma/2 = \varepsilon_d - \alpha$, which we use as a reference energy for the excited states. In CuO, the hybridization shift Γ is smaller, and we shall see below that $\Delta = \varepsilon_p - \varepsilon_d$ has increased to 1 eV.

Recently[7] we consistently interpreted the VB photoelectron spectra (UPS and XPS). Because most of the features in the VB spectra are also reflected in the AES and XES, we will review the assignments here. In the 1:2:3 material, the states were assigned as indicated in Table I.[7,11] In CuO, we have previously assigned a feature at 5.5 eV to pp^{o_a} and pp^p and at 3 eV to dp.[7,12] Calculated photoemission intensities, their variation with Δ, and photon energy dependencies confirm these assignments.[7,13] The character switch of state 1 from mostly dp to pp^p and vice versa for state 2 between CuO and the 1:2:3 material arises because Δ decreases from 1 eV in CuO to near 0 eV in 1:2:3. The reduction in Δ as indicated by the UPS data is consistent with the Cu $2p$ XPS data and with the XES data to be discussed below.

Cu 2p and O 1s core-level XPS. In order to understand the XES and AES data, we first characterize the initial

TABLE I. Summary of hole states revealed in the spectroscopic data, and estimated energies using the indicated optimal values for the Hubbard parameters.

Optimal Hubbard parameter[a] (eV)			
$\delta_1=2$	$\varepsilon_d=2$	$U_p=12, 13$	$U_d=9.5, 10.2$
$\delta_2=0.5, 0.8$	$\varepsilon_p=2, 3$	$U_{pp^o}=4.5, 4$	$U_{dp}=1$
$\Gamma=2$	$U_{pp^p}=0$	$U_{cp^o}=2$	$Q_d=9$
$\alpha=1, 0.5$	$\Delta=0, 1$	$K=4$	

State[b]		Energy expression	Calc. E (eV)[c,d]	Expt. E (eV)[c]	Remark
		g.s., v			
Ψ_a	d	$\varepsilon_d-\delta_1\mp\Gamma$	0 ∓ 2	. . .	Heavily mixed
Ψ_b	p	$\varepsilon_p+\delta_1\mp\Gamma$	4 ∓ 2	. . .	
		UPS and XES, v^2			
1[e]	pp^p	$\varepsilon_p+\Delta-\delta_2+\alpha$	2.5	2.5	Heavily mixed
2[e]	dp	$\varepsilon_p+U_{dp}+\delta_2+\alpha$	4.5	4.2	
3	pp^{o_a}	$\varepsilon_p+\Delta+U_{pp^o}-\Gamma+\alpha$	5.5	5.0	
4	pp^{o_b}	$\varepsilon_p+\Delta+U_{pp^o}+\Gamma+\alpha$	9.5	9.5	Mystery peak
5	d^2	$\varepsilon_d+U_d+\alpha$	12.5	12.5	Cu satellite
6	p^2	$\varepsilon_p+\Delta+U_p+\alpha$	15	16	
		Cu $2p$ XPS, cv			
	cp	$\varepsilon_c+\Delta+\alpha$	ε_c+1	E_{2p}	Main
	cd	$\varepsilon_c+Q_d+\alpha$	ε_c+10	$E_{2p}+9.2$	Satellite
		O $1s$ XPS, cv			
	cd	$\varepsilon_c+\alpha$	ε_c+1	E_{1s}	Main
	cp^p	$\varepsilon_c+\Delta+\alpha$	ε_c+1	E_{1s}	Main
	cp^9	$\varepsilon_c+\Delta+U_{cp^o}+\alpha$	ε_c+3	$E_{1s}+2$?	Tail
	cp	$\varepsilon_c+\Delta+Q_p+\alpha$	?	?	Not observed
		Cu L_3VV AES, v^3			
	dpp^p	$2\varepsilon_p+2U_{dp}+\alpha$	7	7	2 center feature
	dpp^o	$2\varepsilon_p+U_{pp^o}+2U_{dp}+\alpha$	11.5	. . .	No mixing
	d^2p	$\varepsilon_d+\varepsilon_p+U_d+2U_{dp}-\delta_2+\alpha$	16	15.5	Main feature
	dp^2	$2\varepsilon_p+U_p+2U_{dp}+\delta_2+\alpha$	19.5	18–25	Satellite feature
		Cu $L_3M_{23}V$ AES, cv^2			
	cdp	$\varepsilon_c+\varepsilon_p+Q_d+U_{dp}\mp K+\alpha$	ε_c+9	$E_{3p}+10$	Main, ^1L
			ε_c+17	$E_{3p}+18$	Main, ^3L
	cp^2	$\varepsilon_c+\varepsilon_p+\Delta+U_p+\alpha$	ε_c+15	. . .	Not observed
	cd^2	$\varepsilon_c\propto\varepsilon_d+U_d+2Q_d+\alpha$	$\varepsilon_c+30.5$	. . .	Not observed

[a]Parameters for 1:2:3 indicated first, those for CuO second.
[b]The dominant character in the hybridized states is given.
[c]The Calc. E and Expt. E columns indicate the results for 1:2:3.
[d]The calculated E is defined relative to the ground $v^1(d)$ state energy $=\varepsilon_d-\alpha$. The $v^1(d)$ energy defines the Fermi level.
[e]The dominant character switches as described in the text, and thus the sign in front of δ_2 is the opposite for CuO.

state, which is reflected directly in the Cu $2p$ and O $1s$ XPS data. The primary and satellite features seen in the Cu $2p$ XPS spectrum for CuO (Ref. 14) and the 1:2:3 or La (Refs. 1 and 15) material are known to arise from the cp and cd states, respectively,[3,4] with the energies given in Table I. The relative satellite intensity $I(cp)/I(cd)$ decreases from 0.55 in CuO to 0.37 in 1:2:3.[1] The energy separation, $E(cd)-E(cp)$, increases from 8.7 eV in CuO to 9.2 in 1:2:3.[1,4,6]

The primary (cp) and satellite (cd) wave functions can be written similar to Eq. (1), with the hybridization angle $\theta_c=0.5\tan^{-1}[2t/(\Delta-Q_d)]$.[3] In the sudden approximation, the intensities are proportional to the overlap between the ground-state wave function, ψ_a, and the final states, so that $I(dp)\propto\cos^2(\theta_c-\theta_1)$ and $I(cd)\propto\sin^2(\theta_c-\theta_1)$.[3] Thus the satellite intensity increases with increasing difference between the v and cv hybridization angles. In the ground v state, the hole is shared equally in the p and d orbitals since $\theta_1\approx45°$, in the primary cv state it is mostly in the p orbital since $\theta_c\approx78°$. The changes between CuO and 1:2:3 noted above are just that expected for a decrease in Δ and reflect an increased

covalency in 1:2:3.[1]

The large width of the primary *cp* peak is believed to arise from mixing with the *cd* state.[1,3] The *cd* state has a large width due to the large core-hole, valence-hole interaction; indeed, the satellite actually reveals the *cd* multiplet structure. Evidence that the primary *cp* peak width arises from the *cd* interaction comes from the Cu halide data,[3] which show a direct correlation of the primary *cp* peak width with the satellite *cd* peak intensity. We do not believe that the primary peak width arises from the O *p* bandwidth as proposed by others.[16]

The O 1*s* spectra have been reported by many authors; however, it can be seriously altered by impurities such as OH^- and CO_3^{2-} on the sample surface.[17] Recent data[18] from single-crystal samples of the La material cleaved *in situ* are expected to be reasonably free of impurity effects. The cp^o and cp^p states listed in Table I are believed to account for the tailing off seen in these spectra (this will be positively identified upon examination of the XES data). Consistent with the sudden approximation, the *cp* state is not seen in the O 1*s* XPS because now both the *v* and *cv* states have similar hybridization angles, i.e., the valence hole is mostly in the *d* orbital in both cases.

We will find below that the initial-core shake-up (ICSU) process, which is responsible for the satellites in the XPS noted above, does not produce satellites in the AES or XES data, because the ICSU states generally "relax" to the primary states of the same symmetry before the core-level decay. Such a relaxation is expected when the ICSU excitation energy is larger than the core-level width.[19]

Previously, van der Laan *et al.*[3] suggested the intensity of these ICSU states in the XPS should be quantitatively reflected in the intensity of the Auger satellites found in the $L_{23}VV$ line shapes for the Cu halides. The data do not indicate this however. While $I(cd)/I(cp)$ goes from 0.45 for $CuBr_2$ to 0.8 for CuF_2, the Auger satellite intensity does not increase.[3] We previously[1] indicated that a fraction of these ICSU states probably resulted in Auger satellites for the HTSC's, and that this fraction becomes larger as the covalency of the HTSC material increases. Evidence presented here indicates rather that the ICSU states relax before the core-level decay to states of the same symmetry, provided they have a ICSU excitation energy that is much greater than the core-level width. We believe this to be a general result, at least in the Cu^{2+} materials.

The Cu L_{23} and O-K XES data. The O *K* XES data[2] in Fig. 1(a) confirms our assignment of the O XPS, and clearly shows the dependency of the ICSU state relaxation on the excitation energy and symmetry. The principal XPS peak arises from the *cd* state, and it decays to the *dp* state since the x-ray-emission process is intra-atomic in nature. Therefore the principal O XES peak aligns with the *dp* feature in the UPS as shown in Fig. 1. The cp^o state does not mix with the primary *cd* state; therefore, it does not relax before the decay, but decays directly to the pp^{o_b} (and perhaps a little also to the pp^{o_a}) state. This accounts for the feature around 6.5 eV in the XES, just 3 eV above the pp^{o_b} feature in the UPS. The shift of 3 eV matches the energy difference between the cp^o and *cd*

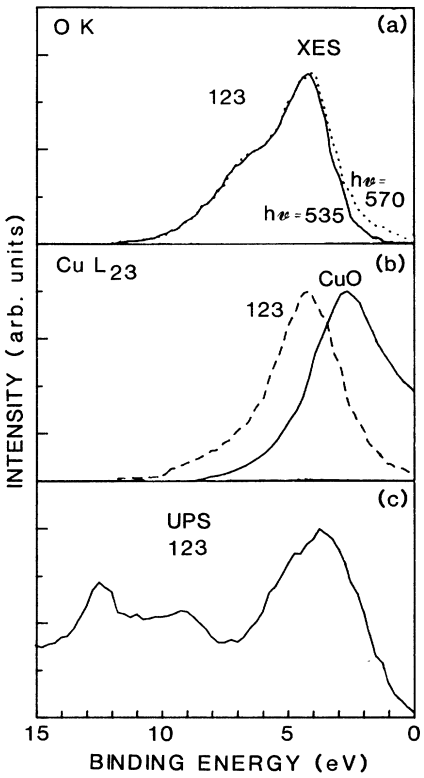

FIG. 1. (a) Comparison of O *K* XES data for 1:2:3 material taken at the indicated photon excitation energies (from Ref. 2). (b) Comparison of Cu L_{23} XES data for 1:2:3 (Ref. 2) and CuO (Ref. 20) material. (c) UPS data for 1:2:3 material ($h\nu = 74$ eV from Ref. 11).

core-hole states. The cp^p state can mix with the *cd* state, therefore it can relax to the *cd* state, but it does this slowly because of the small excitation energy of 0.5 eV. Therefore, the cp^p state decays either directly to the pp^p state, or relaxes to the *cd* state, which then decays to the *dp* state. This explains the photon energy dependence seen[2] in the data of Fig. 1(a). Near threshold, the sudden approximation is not valid, resulting in a smaller intensity for the cp^p state, and consequently a smaller pp^p contribution around 2.5 eV in the XES.

The Cu L_{23} XES data[2,20] shown in Fig. 1(b) dramatically reveals the switch in character of the 1 and 2 v^2 states between CuO and 1:2:3. Again, the satellite *cd* initial state relaxes to the *cp* state before the decay so that the XES reflects primarily the *dp* DOS. In CuO the XES spectrum peaks at 3 eV, in 1:2:3 it falls around 4.2 eV, very near where we indicated the *dp* states fall in the UPS data. The large intensity in the CuO XES extending above the Fermi level is believed to be an experimental artifact.[20]

The Cu $L_{23}VV$ and $L_{23}M_{23}V$ Auger data. Comparison of the L_3VV data for CuO (Ref. 21) and 1:2:3 (Ref. 1) are shown in Fig. 2. The data reveal features at 7 (the two-center feature), 15 (the main feature), and 19 eV (the satellite feature), which we previously[11] attributed to *dp*, d^2, and d^3 final states, respectively, utilizing a v^2

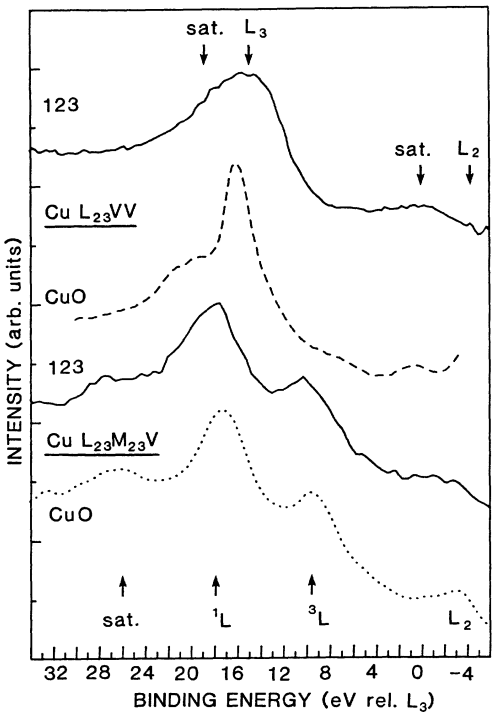

FIG. 2. Comparison of Auger data for the materials indicated. Cu $L_{23}VV$ data for CuO and 1:2:3 from Refs. 21 and 1. Cu $L_{23}M_{23}V$ data for CuO from Ref. 22 and for 1:2:3, this work. The $L_{23}VV$ data are on a two-hole binding energy scale that is equal to $E_{L3}-E_k$, and the $L_{23}M_{23}V$ on a one-hole scale that is equal to $E_{L3}-E_k-E_{M3}$, where $E_{L3}=933.4$ and $E_{M3}=77.3$ eV (Refs. 10 and 12).

final-state model. The d^3 states can arise from 3 different processes: (1) initial core-level shake-off (ICSO) followed by Auger decay (g.s.$+h\nu\rightarrow L_3v\rightarrow d^3$), (2) Coster-Kronig (CK) decay followed by Auger decay (g.s.$+h\nu\rightarrow L_{12}\rightarrow L_3v\rightarrow d^3$), and (3) ICSU followed by Auger decay (g.s.$+h\nu\rightarrow L_3ve\rightarrow L_3v\rightarrow d^3$, where e denotes the excited electron). The ICSO and CK processes accounted for all of the d^3 component in CuO, and the ICSU process was believed, as mentioned above, to account for the increasing satellite d^3 component in the La and 1:2:3 materials.[1]

We report and interpret here, for the first time, the $L_{23}M_{23}V$ Auger line shapes for the 1:2:3 superconductors. The sample preparation, treatment, and instrument utilized were described previously.[1] Figure 2 compares the $L_{23}M_{23}V$ spectra for CuO (Ref. 22) and 1:2:3, and identifies the various features. The $L_{23}M_{23}V$ line shapes reflect the cv^2 DOS in our current cluster model, the main features arising from the cdp final state, and the satellite from the cd^2p state apparently resulting from the similar ICSO, CK, and ICSU processes defined above. However, Fig. 2 reveals a most interesting point; although 1:2:3 shows an increased satellite in the $L_{23}VV$ relative to CuO, it is not increased in the $L_{23}M_{23}V$. This indicates strongly that the ICSU process is not responsible for the increased satellite in the L_3VV, because then it should increase the satellite in both 1:2:3 line shapes.

We indicate that the increase in the $L_{23}VV$ satellite for the HTSC is indeed real. $L_{23}VV$ data for the La and 1:2:3 HTSC's have been reported by several groups,[23] on both sintered polycrystalline and single-crystal samples. Although the relative satellite to main intensity ratio does depend on the extent of impurities on the surface (it is often smaller than that in Fig. 2), it is always larger than that for CuO material. Recent data for the new Bi and Th HTSC's show a similar trend.[24]

Since only the primary cp core-hole state Auger decays, and this process is also known to be strictly intra-atomic, the $L_{23}VV$ line shape in our current v^3 final-state model reflects the d^2p DOS, as it is distributed among the v^3 states listed in Table I. Thus the features at 7, 15, and 19 eV arise naturally from the dpp^p, d^2p, and dp^2 final states. The ICSO and CK processes also contribute to the "satellite" contribution at 19 eV just as in CuO. The dpp^o state does not appear in the L_3VV line shape because it does not have the same symmetry possessed by all the other v^3 final states and the cv initial state. The increased "satellite" feature at 19 eV in the HTSC's arises apparently because of increased configuration mixing between the d^2p and dp^2 states. Its intensity is increased in 1:2:3 relative to CuO because the energy separation (before hybridization) between d^2p and dp^2 has decreased from 3.8 eV in CuO to 2.5 eV in 1:2:3. We have indicated this mixing in Table I by adding the hybridization shifts δ_2 to the energy expressions for these two states.

The $L_{23}M_{23}V$ line shape reflects the cdp DOS. The mixing of the other states (cd^2, cpp^p, cpp^{o_a}, and cpp^{o_b}; the latter three are not listed in Table I) with the cdp state is small because of the large energy separations involved. The cp^2 state is close to cdp; however, it falls in between the ^3L and ^1L multiplets of the cdp state. Although it may have some intensity, it surely does not contribute to the CK+SU satellite around 25 eV in either CuO or 1:2:3. The exchange splitting ($2K$) between the $3p$ and d holes is known to be very large,[3] so we include it explicitly in Table I to account for the $^{1,3}L$ multiplets.

The O KVV line shape can be severely altered by impurities on the HTSC sample surfaces, so we do not consider it here. The O KVV line shapes for CuO and Cu_2O have been reported[12] for samples prepared *in situ*. They have the primary dp^2 or p^2 features, respectively, around 19 eV. A very small satellite appears around 7 eV in Cu_2O which we attribute to the pp^p state. A much larger and broader satellite around 7 to 14 eV in CuO appears, which we attribute to the d^2p state around 14 eV as well as a smaller amount to the dpp^p state around 7 eV. Thus the d^2p and dp^2 states appear in both the Cu $L_{23}VV$ and O Auger line shapes for Cu^{2+} oxides, except their primary and satellite roles are reversed.

In summary, we have interpreted XES and AES data utilizing a highly correlated CuO_n cluster model. Both the XES data and the previously interpreted UPS data reveal the reversal in character of the VB states between CuO and the HTSC's. We have also shown that the initial-core shake-up states evident in core-level XPS do not generally produce satellites in the core emission spectra, because they relax to the primary core states of the same symmetry, provided the ICSU excitation energy is greater than the core-level width.

This work was supported in part by the Office of Naval Research.

[1]D. E. Ramaker *et al.*, Phys. Rev. B **36**, 5672 (1987).
[2]K. L. Tsang *et al.*, Phys. Rev. B **37**, 2293 (1988).
[3]G. van der Laan *et al.*, Phys. Rev. B **23**, 4369 (1981); G. A. Sawatzky *et al.*, Phys. Rev. Lett. **53**, 2339 (1985); J. Zaanen *et al.*, Phys. Rev. B **33**, 8060 (1986).
[4]Z Shen *et al.*, Phys. Rev. B **36**, 8414 (1987).
[5]A. Fujimori *et al.*, Phys. Rev. B **35**, 8814 (1987).
[6]J. C. Fuggle *et al.*, Phys. Rev. B **37**, 1123 (1988).
[7]D. E. Ramaker, this issue, Phys. Rev. B **38**, 11816 (1988).
[8]R. A. de Groot, H. Gutfreund, and M. Weger, Solid State Commun. **63**, 451 (1987); W. Folkerts *et al.*, J. Phys. C **20**, 4135 (1987); A. Manthiram, X. X. Tang, and J. B. Goodenough, Phys. Rev. B **37**, 3734 (1988).
[9]J. Redinger *et al.*, Phys. Lett. **124**, 463 (1987); **124**, 469 (1987).
[10]M. R. Thuler, R. L. Benbow, and Z. Hurych, Phys. Rev. B **26**, 669 (1982).
[11]N. G. Stoffel *et al.*, Phys. Rev. B **37**, 7952 (1988); **38**, 213 (1988).
[12]C. Benndorf *et al.*, J. Electron. Spectrosc. Relat. Phenom. **19**, 77 (1980).
[13]R. Kurtz *et al.*, Phys. Rev. B **35**, 8818 (1987).
[14]A. Rosencwaig and G. K. Wertheim, J. Electron. Spectrosc. Relat. Phenom. **1**, 493 (1972/73).
[15]P. Steiner *et al.*, Z. Phys. B **67**, 497 (1987).
[16]D. D. Sarma, Phys. Rev. B **37**, 7948 (1988).
[17]S. L. Qiu *et al.*, Phys. Rev. B **37**, 3747 (1988); W. K. Ford *et al.*, *ibid.* **37**, 7924 (1988); D. E. Ramaker, in *Thin Film Processing and Characterization of High Temperature Superconductors,* edited by J. M. Harper, R. S. Colton, and L. C. Feldman, American Vacuum Society Series No. 3 (American Institute of Physics, New York, 1988), p. 284.
[18]T. Takahashi *et al.*, Phys. Rev. B **37**, 9788 (1988).
[19]J. W. Gadzuk and M. Sunjic, Phys. Rev. B **12**, 524 (1975).
[20]A. S. Koster, Mol. Phys. **26**, 625 (1973).
[21]L. Fiermans, R. Hoogewijs, and J. Vennik, Surf. Sci. **47**, 1 (1975).
[22]P. E. Larson, J. Electron. Spectrosc. Relat. Phenom. **4**, 213 (1974).
[23]D. van der Marel *et al.*, Phys. Rev. B **37**, 5136 (1988); N. Nucker *et al.*, Z. Phys. B **67**, 9 (1987); Phys. Rev. **37**, 5158 (1988); Z. Iqbal *et al.*, J. Mater. Res. **2**, 768 (1987).
[24]J. Weaver and P. Steiner (private communication).